JOURNAL OF MATERIALS SCIENCE 26 (1991) 1867–1872

Ion-induced interfacial mixing in Al/Pd bilayers: incident ion energy and film thickness dependence

C. N. WHANG, J. H. SONG, S. S. KIM, S. O. KIM, H. J. KANG*
Department of Physics, Yonsei University, Seoul 120-749, Korea
R. J. SMITH
Department of Physics, Montana State University, Bozeman, Montana 59717, USA

The dependence of ion beam mixing on the incident ion energy and film thickness in the Al/Pd system are investigated through both experiment and Monte Carlo simulation based on cascade mixing. It is found that the optimum film thickness is the mean damage depth and the degree of mixing increases with increasing incident ion energy. The radiation-enhanced diffusion or thermochemical driving force is found to play an important role, even in the low-energy region (< 40 keV).

1. Introduction

Direct ion implantation and ion beam mixing (IBM) techniques can be used to improve the mechanical and/or chemical properties of a surface. The concentration of implanted ions attainable by direct ion implantation is, however, limited by the sputtering that occurs at the surface during ion bombardment. In such a situation, the ion beam mixing technique is the preferred choice for attaining a high surface concentration of beneficial elements, since it is not limited by sputtering. This IBM process is of considerable interest for basic research and technological applications such as the formation of silicide [1], equilibrium compounds and metastable alloys [2].

Hung and co-workers [3, 4] reported ion-induced amorphous and crystalline phase formation in Al/Ni, Al/Pd and Al/Pt systems. They used multilayered samples which allow for rather well-defined concentration. They did not, however, comment on the basic process of IBM. The complexity of the phenomenon calls for further experimental effort and theoretical study. A first step towards comprehension of the mixing of metal multilayers requires a study of the mixing phenomenon in only one interface, i.e. a bilayered system. Moreover, in the IBM process, it is known that the effective thickness of the deposited layer and the ion beam characteristics are initially selected to give maximum energy deposition at the interface between overlayer and substrate to enhance interfacial mixing. However, only a few results [5, 6] have been reported for the film thickness and energy dependencies of the IBM process. In practice, it is very important to select an optimum combination of the thickness of the overlayer film and the incident ion energy in order to obtain a large mixing yield.

Previously we reported [7] the basic mechanisms involved in the IBM process in the Al/Pd bilayer system. The present study is intended to elucidate the film thickness and incident energy dependencies of the IBM process. The amount of mixing at the interface was investigated by Rutherford back-scattering spectroscopy (RBS) and Auger electron spectroscopy (AES). The experimental results for mixing are qualitatively compared with Monte Carlo simulation results based on isotropic cascade mixing.

2. Experimental procedure

A clean slide glass was placed in a specially designed chamber for *in situ* evaporation and ion beam mixing. A 20 nm thick palladium layer (bottom layer) and a 40 to 90 nm thick layer of aluminium (top layer) were deposited on glass at a rate of 0.1 nm sec^{-1} and then irradiated with Ar^+ to induce interfacial mixing. Mixing was carried out at a base pressure of 2×10^{-7} torr at room temperature. To avoid sample heating due to ion bombardment, the substrate was glued on a large copper heat sink. The incident energy of Ar^+ was varied from 20 to 80 keV. The irradiation dose was fixed at 1×10^{16} cm^{-2} with a flux of 0.5 μA cm^{-2}.

AES depth profiles were used to measure the mixing efficiency. The primary electron energy and the modulation voltage were maintained at 3 keV and 2.2 eV peak to peak, respectively. AES depth profiles were obtained using 1 keV Ar^+ sputter-etching, with simultaneous monitoring of the Al LVV (67 eV) and Pd MNN (330 eV) AES lines.

The RBS technique was employed to evaluate an accurate film thickness of evaporated aluminium and palladium layers and the sputtering rate during

* *Present address*: Department of Physics, Chungbuk University, Cheongju, Korea.

0022–2461/91 $03.00 + .12

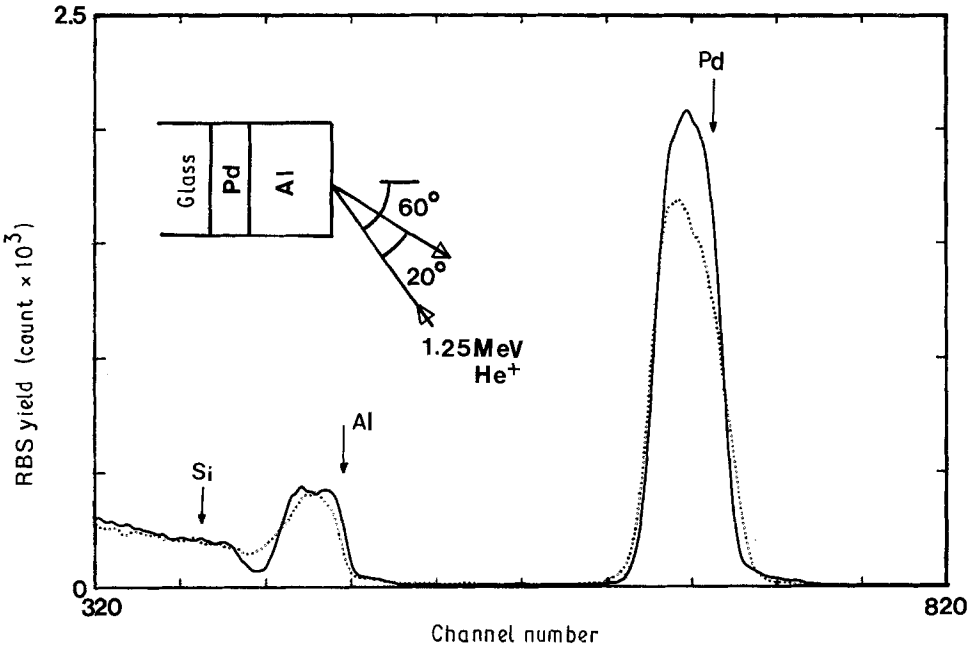

Figure 1 RBS spectra (1.5 keV per channel) of Al(60 nm)/Pd(20 nm) bilayer (——) before and (· · ·) after irradiation with 1×10^{16} Ar^+ cm^{-2}.

AES depth profiling with a 3 keV Ar^+ beam of 25 $\mu A\,cm^{-2}$. An He^+ beam extracted from a 2 MeV Van de Graaff accelerator [8] was magnetically analysed with a solid-state detector at a laboratory scattering angle of 160°. The energy resolution of the analysing system is 15 keV.

3. Results and discussion

3.1. Experimental results of interfacial mixing

Fig. 1 shows typical RBS spectra of Al(60 nm)/Pd for an as-deposited sample and one irradiated with a dose of 1×10^{16} cm^{-2} at an incident energy of 80 keV. The incident energy of He^+ for RBS was 1.25 MeV and the target was tilted to an angle of 60° for better depth resolution. All of the spectra have been normalized to a random glass spectrum obtained from an as-deposited sample. The signals for various elements are indicated by arrows in the figure. It can be seen from Fig. 1 that Ar^+ ion bombardment has caused a broadening of the RBS spectra for palladium and aluminium. It is also apparent that the signal height for palladium is reduced after Ar^+ bombardment, presumably due to the redistribution of atoms through the interface. In addition the rear-edge portion of the aluminium signal moves to lower energy, while the front edge of the palladium signal moves to higher energy after Ar^+ bombardment. This result clearly indicates that intermixing has occurred across the Al/Pd interface as a result of Ar^+ bombardment. The deposited film thicknesses of the aluminium and palladium layers were evaluated using computer simulation [9]. The deposited film thicknesses of aluminium and palladium were found to be 60 and 20 nm, respectively.

The ion beam mixing of an Al(60 nm)/Pd layer, as observed by AES depth profiling, is shown in Fig. 2 along with that of an as-deposited film for comparison. The AES signal of palladium for the mixed sample is normalized to the peak position of palladium in the signal for the as-deposited sample for comparison with each other. After Ar^+ bombardment, the aluminium signal for the interface broadens toward the palldium side, while the palladium signal broadens toward the surface (aluminium side), giving the same trend as the RBS result. Auger line-shape analysis in the mixed region reveals a chemical shift of the 67 eV peak (LVV transition) to a value of 65 eV (not shown in this paper), presumably associated with PdAl compound formation [7].

Comparing Figs 1 and 2 for the as-deposited film, the sputtering rates for aluminium and palladium under 1 keV Ar^+ during AES depth-profiling are found to be 4.42 and 5.02 nm min^{-1}, respectively. The average sputtering yields for the unmixed sample are found to be 2.8 and 3.6 atoms per ion for the aluminium and palladium layers, respectively. The calculated sputtering yields for aluminium and palladium

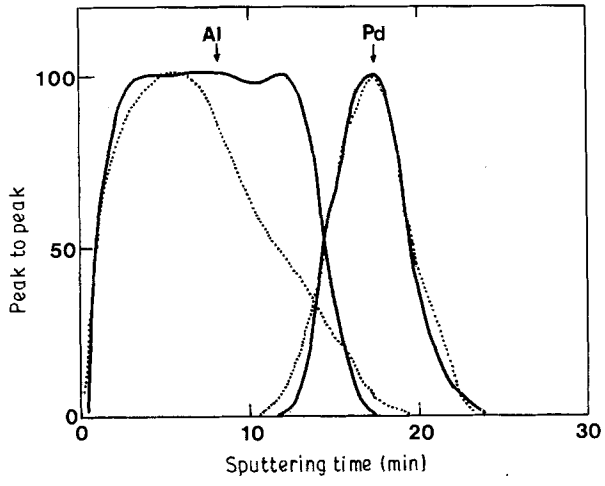

Figure 2 AES depth profiles of Al(60 nm)/Pd(20 nm) bilayer for (——) an unirradiated sample and (· · ·) a mixed sample irradiated with a dose of 1×10^{16} Ar^+ cm^{-2}.

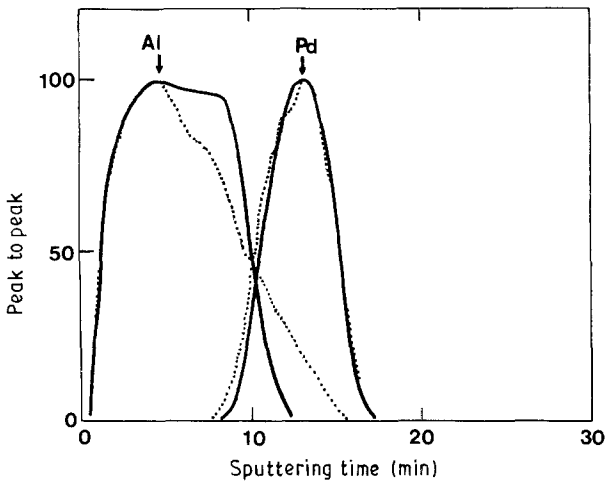

Figure 3 AES depth profiles of Al(40 nm)/Pd(20 nm) bilayer for (——) an unirradiated sample and (· · ·) a sample irradiated with a dose of $1 \times 10^{16} Ar^+ cm^{-2}$.

with 1 keV Ar^+ using an analytical expression [10] are found to be 1.9 and 3.2 atoms per ion, respectively. The experimentally determined sputtering yields are larger than the analytically calculated ones. Exact explanation of this discrepancy is very complicated because of preferential sputtering at the interface. We use the experimental results for sputtering yield for further sputtering depth calibration.

Fig. 3 shows AES depth profiles of Al(40 nm)/Pd bilayers for the as-deposited state and for a mixed state which received a dose of $1 \times 10^{16} cm^{-2}$ at an energy of 80 keV. The spreading of the aluminium and palladium signals at the interface is less than for the Al(60 nm)/Pd sample shown in Fig. 2. Above a thickness of 100 nm for the aluminium layer, the spreading of the aluminium and palladium signals after Ar^+ bombardment is negligible. These results show the film thickness dependency of the ion beam mixing efficiency.

In this paper, our intent is to elucidate the dependence of the ion beam mixing efficiency on film thickness and incident ion energy. The degree of mixing can be represented by the degree to which the AES spectral area spreads across the interface, if sputtering does not occur during ion beam mixing. This method, however, does not work because of sputtering as can be seen in Fig. 2, where the total spectral area of the aluminium signal after ion mixing is reduced due to sputtering. Instead, the amount the intermixing due to Ar^+ bombardment will be characterized by the increase in the variance, Ω^2 of the AES signals for aluminium and palladium:

$$\Omega^2 = \Omega^2(\phi) - \Omega^2(0) \quad (1)$$

where $\Omega(\phi)$ and $\Omega(0)$ are deduced by measuring the half-width between the 16% and 84% points of the AES signals for aluminium and palladium at the interface, for the irradiated, for the irradiated (dose ϕ) and as-deposited (dose 0) sample. Then the variance is converted to units of length using the experimentally determined sputtering yield. The experimental results for aluminium for various aluminium film thickness are shown in Fig. 4. The mixing variance has a maximum value at a thickness of 60 nm for the aluminium layer.

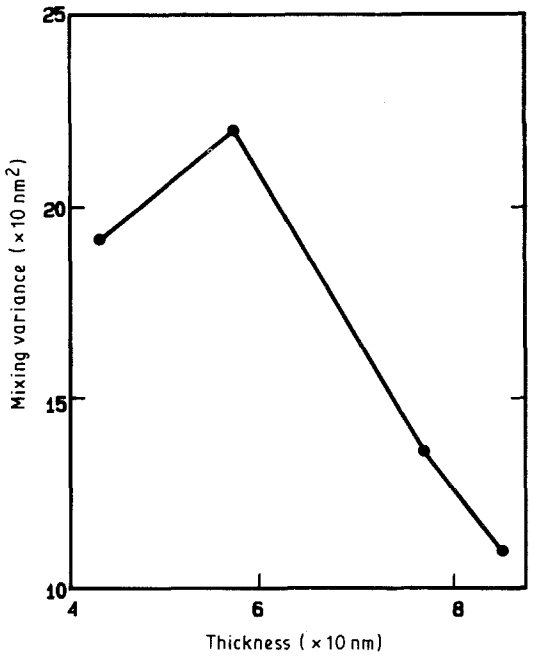

Figure 4 Experimental results of mixing variances for aluminium atoms as a function of thickness of the aluminium layer. The Ar^+ ion energy and dose for mixing are 80 keV and $1 \times 10^{16} Ar^+ cm^{-2}$, respectively.

Fig. 5 shows AES depth profiles of Al(80 nm)/Pd for an as-deposited sample and samples irradiated with incident energies of 20 and 80 keV for a dose of $1 \times 10^{16} cm^{-2}$, and Fig. 6 shows the experimental mixing variances for various incident Ar^+ energies. These results clearly show that the amount of intermixing for aluminium and palladium increases linearly with increasing Ar^+ incident energy. The mixing variance of aluminium is larger than that of palladium, even at the low energy of 20 keV.

3.2. Monte Carlo simulation of interfacial mixing

Computer simulation is probably the most powerful approach for the basic study of IBM. In this study, a

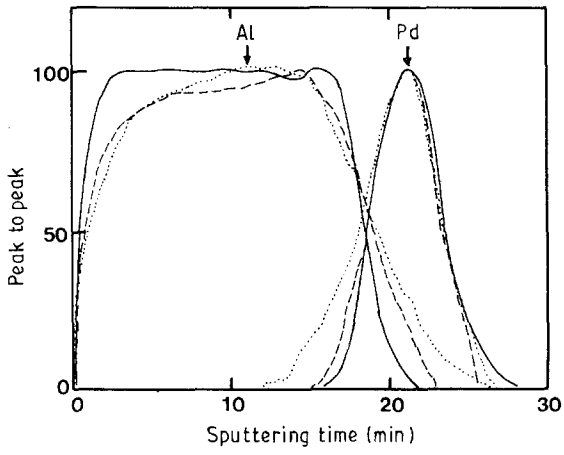

Figure 5 AES depth profiles of Al(80 nm)/Pd(20 nm) bilayer for (——) an unirradiated sample and samples irradiated with (– – –) 20 keV Ar^+ and (· · ·) 80 keV Ar^+. The Ar^+ ion dose is fixed at $1 \times 10^{16} Ar^+ cm^{-2}$.

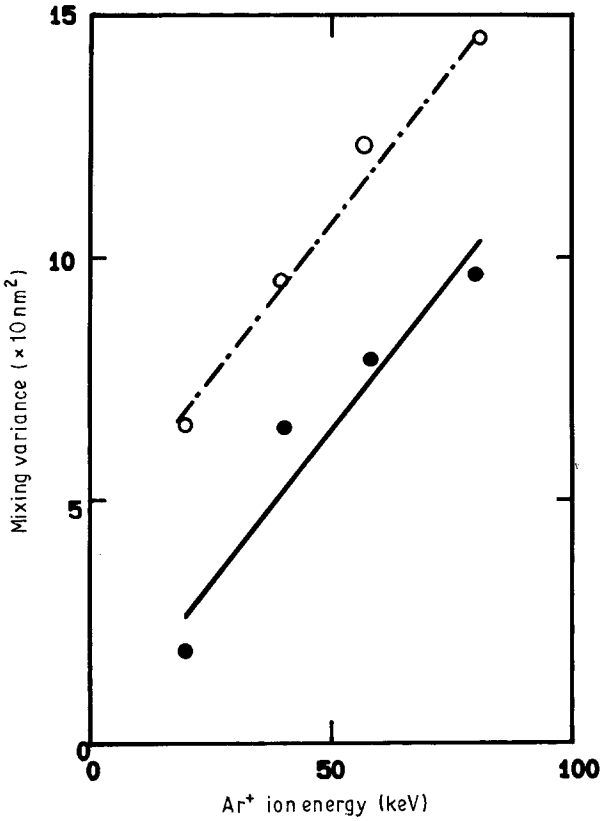

Figure 6 Experimental results of mixing variance for aluminium (–·–) and palladium (——) as a function of the incident Ar^+ ion energy. These results are evaluated from AES depth profiles of Al(80 nm)/Pd(20 nm) bilayers.

computer simulation based on the Monte Carlo technique is developed to elucidate the mechanisms of the interfacial mixing process and applied to the Pd/Al bilayer system for comparison with the present experimental results. It has the advantage [11] of offering physical pictures and proves to be an effective means of obtaining valuable information about mixing. The effects of an interface barrier and cascade mixing are also considered in this simulation. This computer simulation model is based on the binary collision approximation for nuclear stopping and the continuous slow-down energy loss approximation for electronic stopping of an ion penetrating into a solid. Since the basis of this model has already been described in detail elsewhere [12], we briefly describe only the present Monte Carlo simulation of the IBM process.

The Ziegler–Biersack potential is adopted for elastic scattering between colliding atoms because this potential describes the interatomic potential very well, particularly in the low-energy region as confirmed by recent experiments [13, 14]. The electronic energy loss (ΔE_e) in the low-energy region ($E/M \leq 10$ keV a.m.u.$^{-1}$) is described by the Lindhard formula [15] where it is linearly proportional to the velocity of the penetrating ion;

$$S_L = kE^{1/2}$$

$$k = (1.216 \times 10^{-2}) \frac{Z_1^{7/6} Z_2}{M_1^{1/2}(Z_1^{2/3} + Z_2^{2/3})^{3/2}} \quad \text{eV}^{1/2}\,\text{nm}^2 \quad (2)$$

$$\Delta E_e = NS_L l$$

where N is the atomic density and l is the step length or distance between successive elastic collisions. For the high-energy region ($E/M > 10$ MeV a.m.u.$^{-1}$), the modified Bethe–Bloch formula [16, 17] is known to be valid;

$$S_H = \frac{8\pi Z_1^2 eN}{I_0 \varepsilon_B} \ln\left(\varepsilon_B + 1 + \frac{C}{\varepsilon_B}\right) \quad (3)$$

$$\Delta E_e = NS_H l$$

with $\varepsilon_B = 2m_e v^2/Z_2 I_0$, where m_e is the electron mass, $Z_2 I_0$ is the average excitation energy, and $C = 5$ or $C = 100 Z_1/Z_2$ for $Z_1 < 3$. For the medium-energy region, the interpolation scheme [17] is useful:

$$S_M = (S_L^{-1} + S_H^{-1})^{-1}$$

$$\Delta E_e = NS_M l \quad (4)$$

The incident ion loses its kinetic energy through both inelastic collisions with atomic electrons and elastic collision with randomly distributed target atoms. The recoil atom, which receives more kinetic energy than the threshold displacement energy (E_d) through elastic collision, undergoes successive collision processes as does the incident ion until its kinetic energy becomes less than a certain cut-off energy (E_c). If these recoil atoms obtain a high enough energy to generate other recoil processes, this causes high-order recoils leading to the so-called collision cascade. Those recoil atoms which reach the surface with kinetic energy greater than the surface barrier energy (u_s) leave the surface, and are called sputtered atoms. When a collision cascade takes place at the interface of a bilayer system, an intermixed layer is formed at the interface due to the recoiled atoms.

In this simulation for the Al/Pd system, the following parameters are used; $E_c = E_d$, $u_s = 3.36$ eV, $E_d = 16.5$ eV for aluminium and $E_d = 26$ eV for palladium [18, 19]. The total thickness of the Al/Pd bilayer system is divided into a large number of layers (2 nm per layer). All of the collisional processes such as cascade mixing, sputtering and depth distribution of the implanted ions are simulated with 1000 incident Ar^+ ions. In this simulation, we vary the deposited aluminium film thickness from 20 to 100 nm to investigate the optimum film thickness for ion beam mixing at a fixed Ar^+ incident energy of 80 keV, and also vary the incident ion energy from 20 to 100 keV with a fixed aluminium film thickness of 80 nm.

Fig. 7 shows the simulated distribution of vacancies and intermixed aluminium atoms (Fig. 7a) and palladium atoms (Fig. 7b) after 80 keV Ar^+ bombardment into the Al(40 nm)/Pd system. The vacancy distribution is broader than that of intermixed atoms. Quantitatively, 90% of the intermixed atoms come from the layer within a distance of 4 nm from the interface. The total numbers of intermixed aluminium and palladium atoms are 3801 and 3015 atoms, respectively, and the maximum mixing lengths for aluminium and palladium atoms are 20 and 16 nm, respectively. The total number of vacancies resulting from displaced aluminium atoms is larger than that produced by

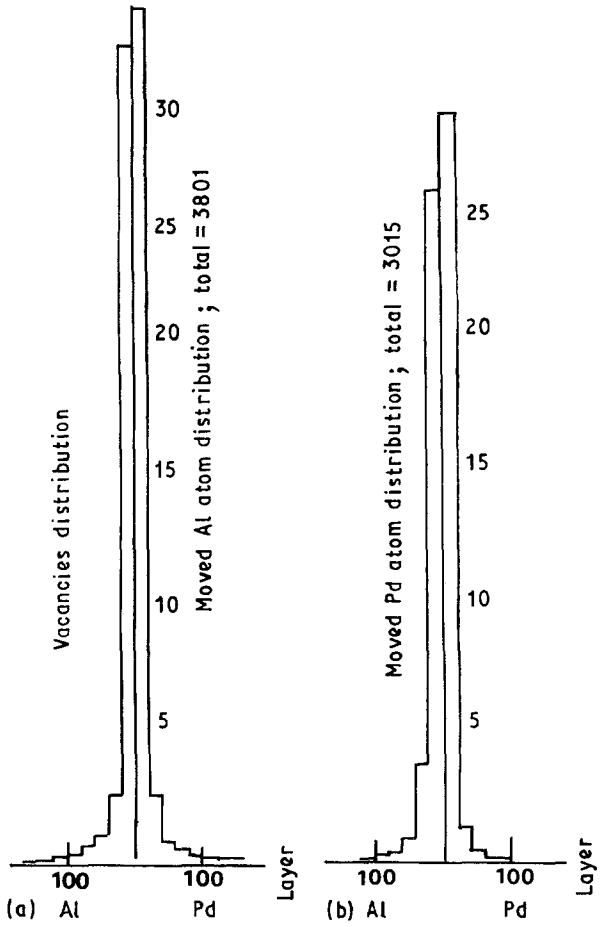

Figure 7 Monte Carlo simulation results for the distribution of vacancy-displaced (a) aluminium and (b) palladium atoms due to 80 keV Ar^+ bombardment in an Al(40 nm)/Pd bilayer.

displaced palladium atoms. These simulation results show that the ion mixing enhances the movement of the lighter species, that is, the lighter atom plays the role of the dominant moving species in a cascade process during ion mixing, which is in good agreement with our previous experimental results [7].

Fig. 8 shows the simulation results for the mixing amounts of aluminium and palladium atoms as a function of aluminium film thickness. In this case, we did not take account of sputtering during ion mixing. The mixing amount reaches a maximum value at a thickness of 40 nm, while the experimental results show that the maximum mixing amount is observed at a thickness of 60 nm. It has been found [7] that the thickness of aluminium sputtered by an ion dose of 1×10^{16} cm^{-2} with an incident energy of 80 keV was 10 nm from RBS area analysis for aluminium, and this increased with ion dose. Therefore, assuming a sputtered layer of 10 nm, the real thickness of the aluminium layer becomes 50 nm after ion mixing, which is close to the simulation result. The mean projected range of the incident Ar^+ and the mean damage depth are found to be 77 ± 28 and 45 ± 5 nm, respectively, from this simulation. The experimental and simulated results show that the optimum film thickness to get the maximum ion mixing yield is close to the mean damage depth.

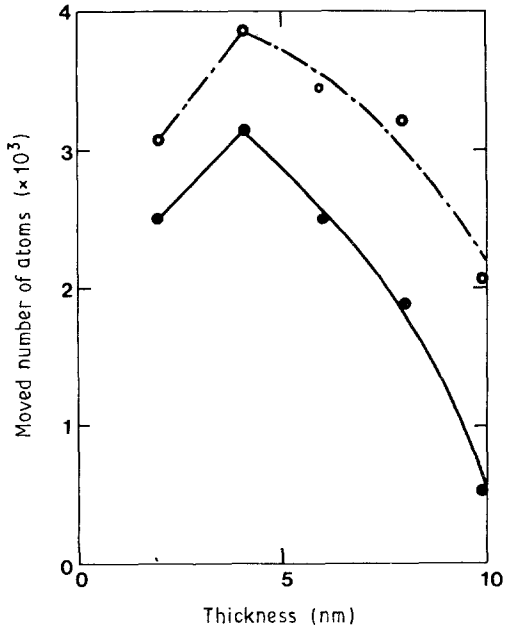

Figure 8 Monte Carlo simulation results for the number of displaced (—·—) aluminium and (——) palladium atoms as a function of thickness of the aluminium layer at the Al–Pd interface due to 80 keV Ar^+ bombardment.

The simulated incident energy dependence of ion beam mixing is shown in Fig. 9. The amount of mixing increases with increasing Ar^+ incident energy, which agrees qualitatively with the experimental results. There is, however, a discrepancy with the experimental results at low energies below 40 keV. In the simulation results, the mixing amount is negligible below 40 keV, while the experimental results show a relatively large amount of mixing. This discrepancy may arise from the mixing mechanisms involved in the IBM process.

Ion bombardment may greatly enhance the diffusion of substitutional or interstitial atoms. The increased vacancy concentration causes a pronounced

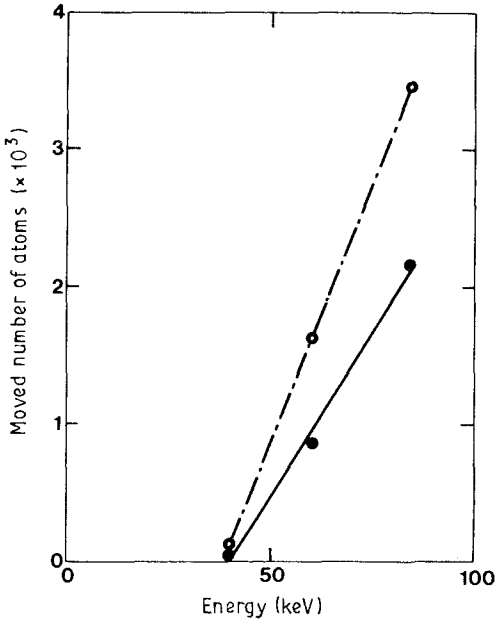

Figure 9 Monte Carlo simulation results for the number of displaced (—·—) aluminium and (——) palladium atoms as a function of incident energy across the interface of an Al(80 nm)/Pd bilayer.

increase in diffusion by the vacancy mechanism, which is usually referred to as radiation-enhanced diffusion (RED) [20]. At lower temperatures below the RED region, isotropic cascades are known to contribute to the short-range mixing. In addition, Cheng *et al.* [21] recently derived a phenomenological equation for the effective diffusion rate, based on the thermochemical properties of the mixing species for a system which has a relatively high heat of mixing enthalpy. The qualitative tendencies for energy dependency, dose dependency and thickness dependency in those mechanisms are the same, but the quantitative mixing amounts show great differences; that is, the diffusion constants based on RED and the thermochemical mechanism are higher than those of the cascade mixing mechanism by an order of 2 and 1, respectively, in the Al/Pd system [7]. Previously we reported [7] that the ion beam mixing mechanisms for aluminium and palladium are RED and thermochemical and/or cascade mixing effects, respectively. The experimental results for energy dependence as shown in Fig. 6 show that relatively large amounts of mixing take place even at low energy, which means that an interfacial mixing process due to RED or a thermochemical mechanism must take place even at low energy. In order to interpret this amount of mixing, a computer simulation including RED and thermochemical properties is needed.

4. Conclusions

Incident Ar^+ energy and deposited aluminium film thickness dependencies of ion beam mixing in the Al/Pd bilayer system are investigated in this study. AES and RBS results show clearly that intermixing has occurred across the Al–Pd interface as a result of Ar^+ bombardment, and there is strong evidence that the mixing amount is dependent on incident energy and film thickness; the mixing amount has a maximum value at an aluminium layer thickness of 60 nm, and this increases with increasing incident Ar^+ energy.

Computer simulation results based on cascade mixing show that most of the mixed atoms come from a distance within 4 nm of the interface, and the total number of intermixed atoms and maximum mixing length for aluminium are larger than those for palladium, which means that the lighter atom plays the role of the dominant moving species in the cascade region during ion mixing. The simulation results for incident energy and film thickness dependencies are qualitatively similar to the experimental results. The experimental results show that relatively large amounts of mixing, presumably due to RED or a thermochemical effect, take place even at lower energy. It is found that the optimum film thickness to give maximum mixing yield is the mean depth.

Acknowledgements

This study was supported in part by the Korea Science and Engineering Foundation (KOSEF). One of the authors (H. J. K.) wishes to express appreciation to R. Shimizu at Osaka University for valuable discussions in developing the Monte Carlo simulation.

References

1. R. Y. LEE, C. N. WHANG, H. K. KIM and R. J. SMITH, *J. Mater. Sci.* **23** (1988) 2740.
2. B. X. LIE, *Phys. Status Solidi (a)* **94** (1986) 11.
3. L. S. HUNG, M. NASTASI and J. W. MAYER, *Appl. Phys. Lett.* **42** (1983) 672.
4. M. NASTASI, L. S. HUNG and J. W. MAYER, *ibid.* **43** (1983) 831.
5. F. Z. CUI and H. D. LI, *Nucl. Instrum. Meth.* **B7/8** (1985) 650.
6. M. BRUEL, M. FLOCCARI and J. P. GAILLIARD, *ibid.* **182/183** (1981) 93.
7. R. Y. LEE, C. N. WHANG, T. K. KIM, S. O. KIM and R. J. SMITH, *ibid.* **B39** (1989) 114.
8. R. J. SMITH, C. N. WHANG and XU MINGDE, *Rev. Sci. Instrum.* **58** (1987) 2284.
9. H. K. KIM, PhD thesis, Yonsei University (1988).
10. R. SHIMIZU, "Energy Dependence of Sputtering Yields of Monoatomic Solids" (Institute of Plasma Physics, Nagoya University, 1980).
11. T. ISHITAMI and R. SHIMIZU, *Appl. Phys.* **6** (1975) 241.
12. H. J. KANG, E. KAWATOH and R. SHIMIZU, *Jap. J. Appl. Phys.* **24** (1985) 1409.
13. *Idem., ibid.* **23** (1983) 1362.
14. W. HETTERICH, H. DERKS and W. HEILAND, *Appl. Phys. Lett.* **52** (1988) 371.
15. J. LINDHARD, *Phys. Rev.* **124** (1961) 128.
16. J. P. BIERSACK and L. G. HAGGMARK, *Nucl. Instrum. Meth.* **174** (1980) 257.
17. C. VARELAS and J. P. BIERSACK, *ibid.* **79** (1970) 213.
18. S. T. KANG, "Investigation on Basic Problems in Secondary Ion Mass Spectroscopy" (Osaka University, 1978) p. 57.
19. K. A. GSCHNEIDER Jr, *Solid State Phys.* **16** (1964) 275.
20. S. M. MYERS, *Nucl. Instrum. Meth.* **168** (1980) 265.
21. Y. T. CHENG, M. VAN ROSSUM, M. A. NICOLET and W. L. JOHNSON, *Appl. Phys. Lett.* **46** (1985) 610.

Received 18 December 1989
and accepted 14 August 1990